VNU Journal of Science: Mathematics – Physics, Vol. 39, No. 3 (2023) 68-77

VNU Journal of Science: Mathematics - Physics

Journal homepage: https://js.vnu.edu.vn/MaP

Original Article

Direct Control of Pt Film Orientation for Growth of (100)-oriented PZT Films

Bui Nguyen Quoc Trinh*

Vietnam Japan University, Vietnam National University, Hanoi,
Luu Huu Phuoc, Nam Tu Liem, Hanoi, Vietnam
University of Engineering and Technology, Vietnam National University, Hanoi,
144 Xuan Thuy, Cau Giay, Hanoi, Vietnam

Received 11 March 2023
Revised 05 April 2023; Accepted 05 April 2023

Abstract: We investigated highly (100)-oriented PZT films directly grown on Pt films coated on $RuO_2/SiO_2/Si$ substrates via sputtering method. By controlling the preferred (100) orientation volume of the Pt films, we confirmed the effectiveness of high (100) orientation of Pt films suitable for the growth of highly (100)-oriented PZT films. Particularly, as the (100) orientation region of Pt film is larger than 90%, the PZT film with 95% of (100) orientation region can be formed, without using any seed layer as well as epitaxial growth process. We found that a highly (100)-oriented PZT film possesses large grains with a size of 150 nm, and it possesses twice remanent polarization of 58 $\mu C/cm^2$ and coercive electric field of 148 kV/cm with the relatively low leakage current less than 10^{-6} A/cm^2 at the applied voltage of ± 4 V. One can convince that the technological process for highly (100)-oriented PZT films is simple, and it is promising for ferroelectric and piezoelectric applications in wide ranges.

Keywords: Pt, PZT, ferroelectric, thin film, sputtering.

1. Introduction

Ferroelectric thin films have intensively investigated for various applications such as pyroelectric infrared sensors, piezoelectric transducers and actuators and ferroelectric random access memories (FeRAM) [1-3]. Among ferroelectric materials, lead zirconate titanate $Pb(Zr_{1-x},Ti_x)O_3$ (PZT) has been

* Corresponding author.
E-mail address: trinhbnq@vnu.edu.vn

https//doi.org/10.25073/2588-1124/vnumap.4838

well-known as a very promising material owing to large remanent polarization and low coercive field, which is a great selectivity for the application of FeRAM. It has been demonstrated that electrical property of PZT films is dependent on many factors such as film composition [4], effect from oxide conductive electrode [5], and orientation of the films [6]. For the tetragonal PZT film ($x \leq 0.52$), the remanent polarization is maximized by orienting the {100} crystallographic direction, that is, (100)-preferred orientation, normal to the film surface, so that the applied electric field is parallel to the {100} direction. Especially, with $x = 0.52$, which is usually called as a composition at the morphotropic phase boundary, the PZT films possess excellent electrical properties, compared with the other composition [7]. Therefore, controlling the preferred orientation of the tetragonal PZT film to (100) is a key factor to obtain a high-quality film. One of the methods to control the preferred orientation of the PZT film is to control the preferred orientation of the under layer, so that the film can be preferably grown on it. For example, the (100)-oriented PZT film were grown epitaxially on $SrTiO_3$(STO) single crystal wafers [8]. However, based on epitaxial growth process, the production requires expensive cost and complicated technique, which are not favor for any purpose of commercialization. Comparing with the epitaxial growth process, the polycrystalline Pt film has been extensively utilized for the deposition of PZT films, because it is cheaper and requires a simpler process. Unfortunately, since the crystal structure of Pt is face-centered cubic (fcc), the preferred orientation of the Pt film is naturally (111). As a result, if the PZT film was deposited directly on it should be random or (111), but not (100) as expected for the tetragonal PZT film. In order to overcome this difficulty, by the sol-gel or metallo-organic decomposition technique, many researchers succeeded to prepare the (100)-oriented PZT films on the polycrystalline Pt film using special seed layers or changing heating schedule. However, this method makes the film formation more complicated.

Heretofore, except epitaxial growth process, a few researchers reported on the (100)-oriented PZT film derived directly on the polycrystalline Pt film by sputtering method because of the above mentioned difficulties. Previously, we succeeded to deposit a (100)-oriented polycrystalline Pt film, at the low temperature of 100 ^oC on the $RuO_2/SiO_2/Si$ substrates by controlling the oxygen incorporation [9]. As a result, in this work we characterize on the (100)-oriented PZT films directly grown on the Pt films with various orientation without any seed layer.

2. Experimental Procedures

Initially, a 10-nm-thick SiO_2 layer was formed on a Si substrate with a resistivity of 8.5−11.5 Ωcm through dry-oxidation method. Following this, a RuO_2 film and a Pt film were, respectively, deposited for the bottom electrode by sputtering method, whose deposition conditions have been enlisted in Table 1. In this double-layer structure, the thickness of RuO_2 film and Pt film were 60 nm and 200−600 nm, respectively. The RuO_2 film plays an important role to supply oxygen for the ferroelectric film in suppression of fatigue properties. The Pt film is chemically stable to the PZT film deposited on it and has catalytic effect on enhancing the diffusion of oxygen from the RuO_2 film to the PZT film. Importantly, the preferred orientation of the Pt film affects directly on that of the PZT film. At the temperature of 100 ^oC, by altering gas pressure, sputtering power and the film thickness, the preferred orientation of the Pt film was controlled as mentioned above. PZT films were deposited onto the Pt-coated substrates using sputtering at 600 °C so that the orientation dependence of the PZT film on the preferred orientation of the Pt film can be evaluated. The detailed sputtering conditions of the PZT films were also shown in Table 1. For PZT film deposition, in order to maintain a stochiometric content of the lead in the sputtered PZT film, eight 10-mm-diameter PbO pellets were circled on the a 4-inch-diameter $Pb_{1.1}(Zr_{0.52}Ti_{0.48})O_3$ target.

Table 1. Sputtering conditions for deposition of RuO_2 and Pt and PZT films

Films	RuO_2	Pt	PZT
Target	Ru metal	Pt metal	$Pb_{1.1}Zr_{0.52}Ti_{0.48}O_3$ + 8 PbO pellets
Substrate temperature	100 °C	100 °C	600 °C
RF power	50 W	20 W	50 W
Sputtering gas	$Ar/O_2 = 3/1$	Ar	$Ar/O_2 = 9/1$
Working pressure	4 Pa	0.5-10 Pa	0.5 Pa
Thickness	60 nm	200–600 nm	170 nm

The crystalline structure of Pt films and PZT films was investigated by X-ray diffraction (Philips X'Pert system with CuKα radiation). The thicknesses of Pt, RuO_2 and PZT films were measured using a Dektak surface profiler system. Surface roughness and morphology were investigated by atomic force microscopy, NanoNavi/S-image Probe station (SII NanoTechnology Corporation). To evaluate the volume ratio of the oriented region over the whole deposited Pt or PZT film, we used the integrated intensity I_{hkl} from the (*hkl*) plane in the measured XRD pattern. I_{hkl} was corrected by the film thickness because the penetration depth of the X-ray for Pt or PZT film, ~ 2 μm, is greater than the film thickness, < 600 nm [10]. Also, I_{hkl} was normalized by the integrated intensity of Si (400) in order to compensate for fluctuation of the X-ray beam intensity on the diffracted intensity. The detailed calculation was mentioned in our previous work [9]. To investigate the ferroelectric properties of the (111)-oriented PZT film, top electrodes with 100 μm in diameter were formed by depositing 200-nm-thick RuO_2 film. After that, the polarization vs electric field (*P-E*) hysteresis loops were measured using the RT66A ferroelectric test system (Radiant Technologies. Inc.) with a frequency of 100 Hz. Leakage current density versus voltage (*J-V*) characteristic were measured with step voltages and the time interval of each step was 2 seconds.

3. Results and Discussion

Figure 1 shows XRD patterns of the Pt films deposited on $RuO_2/SiO_2/Si$ substrates. From this figure, one observed that the preferred orientation of the Pt films is gradually changed from (111) to (100). At the temperature of 100 °C, when Pt film thickness is small, about 200 nm, and the pressure is low, about 0.5 Pa, the preferred orientation of the Pt film is dominated to be (111) as shown in Fig. 1(a). This is because the crystal structure of Pt is a face-centered cubic, the (111) plane has largest density of atoms comparing with the other planes, that is, the surface energy of (111) plane is lowest, the preferred orientation of the Pt film is ease to be (111). However, once the film thickness increased and the pressure is higher, the Pt(111) peak is reduced, but the Pt(200) peak increased. In other words, the preferred orientation of the Pt film is switched from (111) to (100) when changing sputtering conditions. In fact, if the pressure of 5 Pa and the thickness of 400 nm are used, the orientation of Pt film is random as shown in Fig. 1(b). When further increment, that is, the pressure is increased to 10 Pa and the thickness is about 600 nm, the preferred orientation of Pt film is (100) according to Fig. 1(c). This result could be explained by considering competition between surface energy and strain energy in the Pt film. The strain energy is increased with the stress and the film thickness of the film, while the surface energy is almost independent on them. Therefore, when the pressure and the film thickness are small, the surface energy becomes more dominant than the strain energy, leading to (111)-preferred orientation. On the contrary, when the pressure and the film thickness increased, the strain energy becomes more dominant than the

surface energy, leading to (100)-preferred orientation. Further explanation on the stress and strain of polycrystalline films can be found in [11].

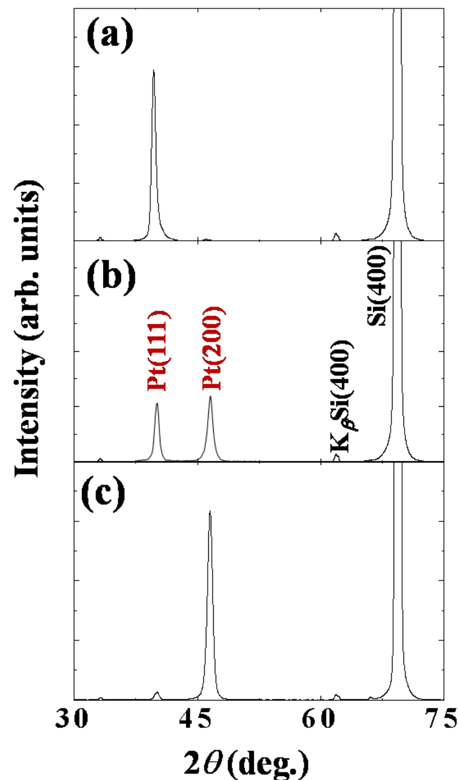

Figure 1. XRD patterns of the Pt films deposited on $RuO_2/SiO_2/Si$ substrates: (a) highly (111)-oriented, (b) randomly oriented and (c) highly (100)-oriented.

Next, we investigated the crystalline structure of the 180-nm-thick PZT films deposited on the highly (111)-oriented, the randomly oriented and the highly (100)-oriented Pt films. Figure 2 shows XRD patterns of PZT thin films deposited on them. One can see that, on the highly (111)-oriented Pt film, the PZT(100) peak is hardly appeared, but the PZT(110) peak is high as shown in Fig. 2(a). Also, from this figure the appearance of small PZT(111) peak can be seen, which means even the (111)-oriented PZT film is hardly grown on the (111)-oriented Pt film because the activation energy of (111) orientation is quite high. Ambika et al., [12] reported that the substrate temperature higher than 650 °C is needed for growth of (111)-oriented PZT film on the (111)-oriented Pt film. On the randomly oriented Pt film, that is, when the (100) orientation volume of Pt film is increased, the PZT(100) peak is increased, but the PZT(110) peak is reduced as shown in Fig. 2(b). Interestingly, on the highly (100)-oriented Pt film with large (100) orientation volume, the PZT(100) peak is abruptly increased, while the PZT(110) and PZT(111) peaks are barely visible as seen from Fig. 2(c). From this result, it is obvious that the (100) preferred orientation of PZT film depends strongly on that of the Pt film. On the other hand, from Fig. 2(c), one concluded that the highly (100)-oriented PZT film can be directly grown on the highly (100)-oriented Pt film at the substrate temperature of 600 °C.

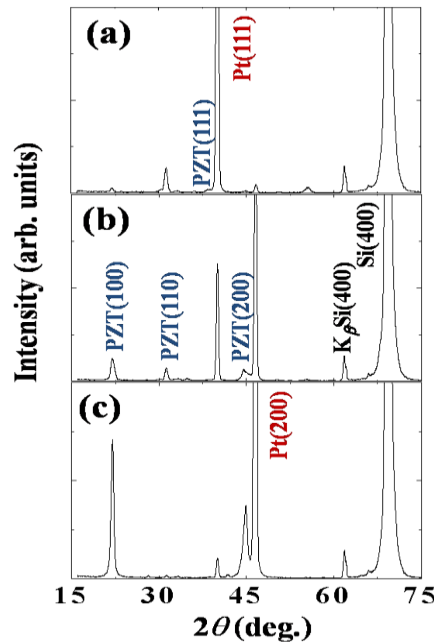

Figure 2. XRD patterns of the PZT films deposited on Pt/RuO_2/SiO_2/Si substrates with: (a) highly (111)-oriented Pt film, (b) randomly oriented Pt film and (c) highly (100)-oriented Pt film.

In order to evaluate the important role of the highly (100)-oriented Pt film in growth process of the (100)-oriented PZT film, we consider the volume ratio of the Pt(100) region and the total region of Pt(100) and Pt(111), α_{Pt}. If the α_{Pt} is near 1, the Pt film is highly (100)-oriented. Otherwise, the Pt film is random or (111)-oriented. Actually, the α_{Pt} is calculated as follows:

$$\alpha_{Pt} = \frac{I_{Pt(100)}}{I_{Pt(100)} + I_{Pt(111)}} \tag{1}$$

where $I_{Pt(100)}$ and $I_{Pt(111)}$ are the corrected integrated intensities for (100) and (111) orientations of Pt film, respectively.

Similarly, for the PZT films deposited on these Pt films, we also calculate the volume ratio between the PZT(100) region and the total region of PZT(100), PZT(110) and PZT(111), α_{PZT}, as following:

$$\alpha_{PZT} = \frac{I_{PZT(100)}}{I_{PZT(100)} + I_{PZT(110)} + I_{PZT(111)}} \tag{2}$$

where $I_{PZT(100)}$, $I_{PZT(100)}$ and $I_{PZT(111)}$ are the corrected integrated intensities for (100), (110) and (111) orientations of PZT film, respectively. The highly (100)-oriented PZT film has α_{PZT} near 1.

Fig. 3 shows the dependence of orientation volume ratio of PZT film (α_{PZT}) on that of Pt film (α_{Pt}). The results indicated that the α_{PZT} is increased with the increment of the α_{Pt}. In particular, if the α_{Pt} is toward zero-side, the PZT film has a tendency to be random orientation. However, when the α_{Pt} is in range of 0.9–1.0, the PZT films have a high (100) orientation, and approaches saturation region. It means that the values of α_{Pt} should larger than 0.9 so that we can derive the highly (100)-oriented PZT film in this work. For the Pt film of Fig. 1(a), we estimated $\alpha_{Pt} \approx 0.01$, corresponded to $\alpha_{PZT} \approx 0.15$ of the PZT

film as shown in Fig. 2(a). Similarly, for Fig. 1(b) and Fig. 2(b), $\alpha_{Pt} \approx 0.5$ corresponded to $\alpha_{PZT} \approx 0.15$; and for Fig. 1(c) and Fig. 2(c), $\alpha_{Pt} \approx 0.94$ corresponded to $\alpha_{PZT} \approx 0.96$. From this result, one can conclude that (100)-oriented PZT film can be only grown on the Pt(100) film with a sufficiently high (100) orientation. In other words, the highly (100)-oriented Pt film plays as a direct seed layer to transfer (100) orientation for the polycrystalline PZT film.

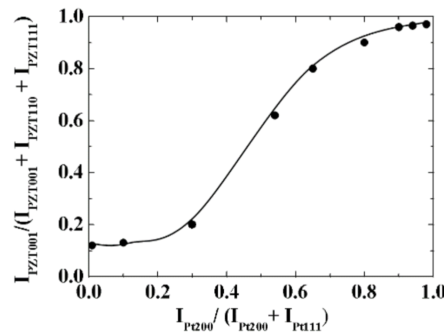

Figure 3. Relationship of the crystalline quality between the Pt films and the PZT films.

Fig. 4 shows atomic force micrograph of the (100)-oriented PZT film with 170 nm thickness derived on the highly (100)-oriented Pt film. One can see that the (100)-oriented PZT film has large grain size about 150 nm and roughness less than 75 nm.

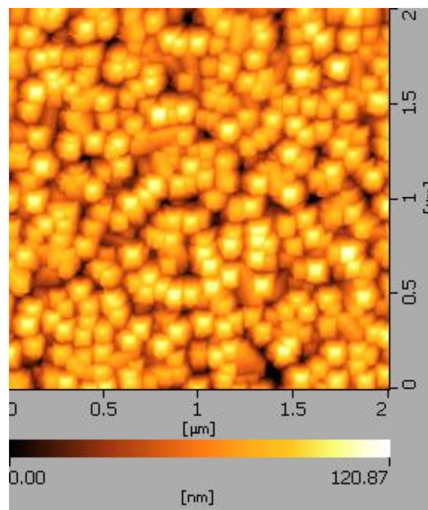

Figure 4. Atomic force micrograph of the highly (100)-oriented Pt film.

Fig. 5(a) shows the typical *P-E* hysteresis loop of the highly (100)-oriented PZT film deposited on the highly (100)-oriented Pt film, corresponding to $\alpha_{Pt} \approx 0.94$ and $\alpha_{PZT} \approx 0.96$. From this figure, one can observe that the *P-E* hysteresis loop possesses good symmetry and square shape and ease to be saturated. According to the hysteresis loop, the twice remnant polarization ($2P_r$), is difference between the positive and the negative polarizations, is estimated to be 58 μC/cm^2. Also, the twice coercive electric field ($2E_c$), is difference between the positive and the negative coercive electric field, is estimated about 148 kV/cm.

In order to evaluate essentially the ferroelectric properties of the (100)-oriented PZT film, we plotted the dependence of $2P_r$ and $2E_c$ on the electric field E as shown in Fig. 5(b). One can see that the remnant polarization and the coercive electric field are saturated around 230 kV/cm.

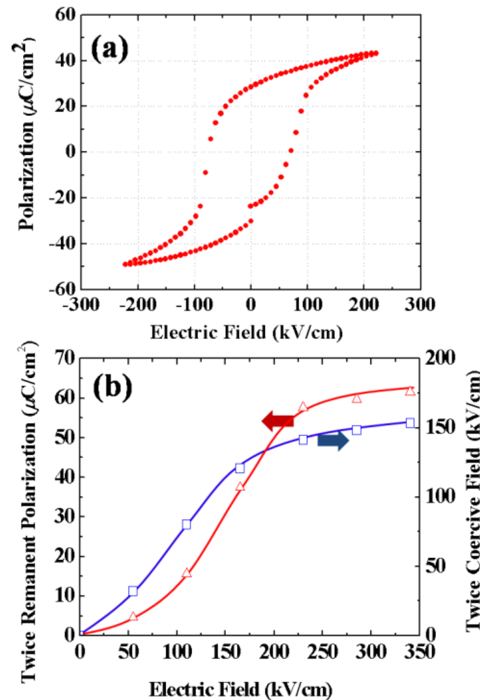

Figure 5. Ferroelectric properties of the (100)-oriented PZT film: (a) polarization versus electric field (b) dependence of the twice remanent polarization ($2P_r$) and the twice coercive field ($2E_c$) on electric field.

Fig. 6 shows the leakage current density versus voltage (J-V) characteristic of the (100)-oriented PZT film. In this case, we measured the non-switching current or the sample was biased at +4 V and –4 V before the measurement of the positive current and the negative current, respectively. In Fig. 7, the leakage-current characteristic of a typical (100)-oriented PZT film is illustrated, revealing a relatively low leakage current at ±4 V of almost 10^{-6} A/cm^2. Due to this leakage current, one can see from Fig. 5(b) that, the $2P_r$ and $2E_c$ are easily approached to the saturation region, and the saturated values of $2P_r$ and $2E_c$ are slightly raised up with increment of electric field. Recently, PZT thin films with piezoelectric properties have been reported [13], In addition, transparent piezoelectric thin-film devices using PZT thin films can be successfully realized [14]. Hence, our achievement on the control of orientation volume can be supportive to the improved piezoelectric properties of the films. Although the $2P_r$ value for the (100)-oriented PZT film in this study is 25% lower than that of the epitaxial PZT film,, its $2E_c$ value is higher. Considering disadvantages of the epitaxial film with the polycrystalline film, the highly (100)-oriented Pt film is more suitable for industry requirements. Furthermore, the hysteresis loop of the polycrystalline PZT of high (100) orientation is symmetrical, i.e., without imprint effect, while that of the expitaxial PZT film is shifted toward the negative side of E which cause serious problem for flexible applications. For the case of epitaxial PZT film, the structure of Au/PZT/Ir ferroelectric capacitor is typically used. However, for the case of polycrystalline PZT with high (100) orientation, the structure of RuO_2/PZT/Pt ferroelectric capacitor is well known. Probably, by using the RuO_2 film for the top

electrode of RuO_2/PZT/Pt capacitor, there is no interfacial layer between the top electrode and the PZT layer, which had high traps and charge centers. It means that the interface between RuO_2 and PZT film is supportive from each other, so that the *P-E* loop of the RuO_2/PZT/Pt capacitor is symmetrical.

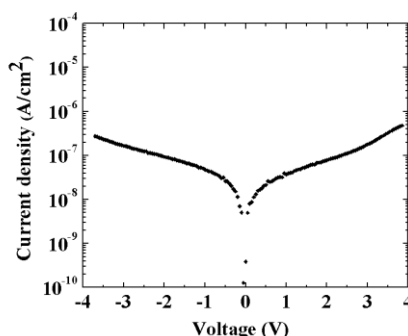

Figure 6. Leakage current density versus voltage characteristic of the (100)-oriented PZT film.

Yu et al., [15] reported that the value of $2P_r$ for the epitaxial (100)-oriented PZT film grown on $LaNiO_3$ is about 52 μC/cm^2, which should be slightly lower than the value obtained from this study. Probably, this is because the stability of Pt thin film is much better than that of $LaNiO_3$ thin film during the crystallization of PZT thin films. S. Yokoyama [16] reported that the (100)-oriented $Pb(Zr_{0.2}Ti_{0.8})O_3$ film grown on an epitaxial $SrRuO_3/SrTiO_3$ substrate had $2P_r \approx 130$ μC/cm^2, which is much higher than our achievement. However, the use of epitaxial $SrRuO_3/SrTiO_3$ substrate requires a high cost comparing with the use of Si substrate, therefore, a trade off should be needed. To our best knowledge, the $2P_r$ is typically about 50-70 μC/cm^2 for the polycrystalline PZT films, which are matched with our achievement results [17-18].

Judging from the archived results of $2P_r$, $2E_c$ and the leakage current, we believe that the highly (100)-oriented PZT film deposited directly on the highly (100)-oriented Pt film has good quality enough for application in FeRAM technology. This has already been demonstrated in our previous work [19] where we utilized this film for a ferroelectric gate field-effect transistor memory with an intermediate electrode (IF-FET). Because of the relatively low leakage current and the adequate remnant polarization, it has been demonstrated that the retention time and reading endurance of the IF-FET memory are 10 years and 10^8 reading cycles, respectively.

4. Conclusion

We investigated the growth process of the (100)-oriented PZT films on the $Pt/RuO_2/SiO_2/Si$ substrates with controlling the preferred orientation volume of the Pt film deposited by sputtering method. When the (100) orientation region of Pt film is considerably large, the (100)-oriented PZT films can be grown directly on the highly (100)-oriented Pt films without using any seed layer as well as epitaxial growth technique. This result suggests that (100)-oriented Pt film plays as a direct seed layer to obtain the (100)-oriented PZT films. The derived highly (100)-oriented PZT film consists of crystalline grains with the size as large as 150 nm, the films possess good ferroelectric properties: a remnant polarization $2P_r$ of 58 μC/cm^2 and coercive electric field of 148 kV/cm with the relatively low leakage current less than 10^{-6} A/cm^2 at the applied voltage of $\pm$ 4 V.

Acknowledgment

This work is fully supported by the project with the code number of VJU.JICA.21.03, from Vietnam Japan University, under Research Grant Program of Japan International Cooperation Agency.

References

[1] J. F. Scott, C.A. P. de Araujo, Ferroelectric Memories, Science, Vol. 246, 1989, pp. 1400-1405, https://doi.org/10.1126/science.246.4936.140.

[2] O. Auciello, J. F. Scott, R. Ramesh, The Physics of Ferroelectric Memories, Phys. Today, Vol. 51, 1998, pp. 22-27, https://doi.org/10.1063/1.882324.

[3] B. N. Q. Trinh, S. Horita, Operation of Ferroelectric Gate Field-Effect Transistor Memory with Intermediate Electrode using Polycrystalline Capacitor and Metal–Oxide–Semiconductor Field-Effect Transistor, Japanese Journal of Applied Physics, Vol. 45, 2006, pp. 7341-7344, https://doi.org/10.1143/JJAP.45.7341.

[4] P. Khaenamkaewa, S. Muensit, I. K. Bdikin, A. L. Kholkin, Effect of Zr/Ti ratio on the Microstructure and Ferroelectric Properties of Lead Zirconate Titanate Thin Films, Materials Chemistry and Physics, Vol. 102, 2007, pp. 159-164, https://doi.org/10.1016/j.matchemphys.2006.11.019.

[5] T. Nakamura, Y. Nakao, A. Kamisawa, H. Takasu, Preparation of $Pb(Zr,Ti)O_3$ thin Films on Electrodes Including IrO_2, Appl. Phys. Lett., Vol. 65, 1994, pp. 1522-1524, https://doi.org/10.1063/1.112031.

[6] C. J. Kim, D. S. Yoon, J. S. Lee, C. G. Choi, K. No, A Study on the Microstructure of Preferred Orientation of Lead Zirconate Titanate (PZT) Thin Films, J. Mater. Res., Vol. 12, 1997, pp. 1043-1047, https://doi.org/10.1557/JMR.1997.0145.

[7] L. Jiankanga, Y. Xia, Microstructure and Electrical Properties o $Pb(Zr_{0.52}Ti_{0.48})O_3$ Ferroelectric Films on Different Bottom Electrodes, Materials Letters, Vol. 58, 2004, pp. 3447-3450, https://doi.org/10.1016/j.matlet.2004.03.053.

[8] H. Ha, B. N. Q. Trinh, Epitaxial-like Growth of Solution-processed $PbZr_{0.4}Ti_{0.6}O_3$ Thin Film on Single-crystal Nb-doped SrTiO3 Substrate, VNU Journal of Science: Mathematics – Physics, Vol. 33, 2017, pp. 36-44, https//doi.org/10.25073/2588-1124/vnumap.4244.

[9] B. N. Q. Trinh, S. Horita, Control of Preferential Orientation of Platinum Films on $RuO_2/SiO_2/Si$ Substrates by Sputtering, Japanese Journal of Applied Physics, Vol. 45, 2006, pp. 8810-8816, https://doi.org/10.1143/JJAP.45.8810.

[10] B. E. Warren, X-ray Diffraction, Dover Publications, New York, 1990.

[11] G. C. A. M. Janssen, Stress and Strain in Polycrystalline Thin Films, Thin Solid Films, Vol. 515, 2007, pp. 6654-6664, https://doi.org/10.1016/j.tsf.2007.03.007.

[12] D. Ambika, V. Kumar, K. Tomioka, I. Kanno, Deposition of PZT Thin Films with {001}, {110}, and {111} Crystallographic Orientations and Their Transverse Piezoelectric Characteristics, Adv. Mat. Lett., Vol. 3, 2012, pp. 102-106, https://doi.org/10.5185/amlett.2011.7281.

[13] G. Tan, S. H. Kweon, I. Kanno, Piezoelectric Properties of Epitaxial $Pb(Zr,Ti)O_3$ Thin Films Grown on Si Substrates by the Sol–gel Method, Thin Solid Films, Vol. 764, 2023, pp. 139612, https://doi.org/10.1016/j.tsf.2022.139612.

[14] K. Ueda, S. H. Kweon, H. Hida, Y. Mukouyama, I. Kanno, Transparent Piezoelectric Thin-film Devices: $Pb(Zr,Ti)O_3$ Thin Films on Glass Substrates, Sensors and Actuators A: Physical, Vol. 327, 2021, pp. 112786, https://doi.org/10.1016/j.sna.2021.112786.

[15] Y. Yu, M. Lai, L. Lu, Highly (100) Oriented $Pb(Zr_{0.52}Ti_{0.48})O_3/LaNiO_3$ Films Grown on Amorphous Substrates by Pulsed Laser Deposition, Appl. Phys. A, Vol. 88, 2007, pp. 365-370, https://doi.org/10.1007/s00339-007-3968-y.

[16] S. Yokoyama, Y. Honda, H. Morioka, S. Okamoto, T. Iijima, H. Matsuda, K. Saito, H. Funakubo, Comparison Study of (001)-/(100)-Oriented Epitaxial and Fiber Textured $Pb(Zr,Ti)O_3$ Thick Films Prepared by MOCVD, Integrated Ferroelectrics, Vol. 64, 2004, pp. 217-225, https://doi.org/10.1080/10584580490894366.

[17] R. Thomas, S. Mochizuki, T. Mihara, T. Ishida, Preparation of $Pb(Zr,Ti)O_3$ Thin Films by RF-magnetron Sputtering with Single Stoichiometric Target: Structural and Electrical Properties, Thin Solid Films, Vol. 413, 2002, pp. 65-75, https://doi.org/10.1016/S0040-6090(02)00354-1.

[18] C. C. Mardare, E. Joannia, A. I. Mardare, J. R. A. Fernandes, C. P. M. de Sa´, P. B. Tavarese, Effects of Adhesion Layer (Ti Or Zr) and Pt Deposition Temperature on the Properties of PZT Thin Films Deposited by RF Magnetron Sputtering, Applied Surface Science, Vol. 243, 2005, pp. 113-124, https://doi.org/10.1016/j.apsusc.2004.09.050.

[19] S. Horita, B. N. Q. Trinh, Disturb-Free Writing Operation for Ferroelectric-Gate Field-Effect Transistor Memories with Intermediate Electrodes, IEEE Transactions on Electron Devices, Vol. 56, 2009, pp. 3090-3096, https://doi.org/10.1109/TED.2009.2032744.